IEA Wind Task 46

Erosion of wind turbine blades

Rain erosion test data analysis, damage accumulation and VN curves

Technical report

Jamie Engelhardt Simon and
Nicolai Frost-Jensen Johansen

iea win

Technical Report

D4.3 Rain erosion test data analysis, damage accumulation and VN curves

Prepared for the International Energy Agency Wind Implementation Agreement

December 2024

Purpose

Leading edge erosion (LEE) of wind turbine blades has been identified as a major factor in decreased wind turbine blade lifetimes and energy output over time. Accordingly, the International Energy Agency Wind Technology Collaboration Programme (IEA Wind TCP) has created the Task 46 to undertake cooperative research in the key topic of blade erosion. Participants in the Task are given in Table 1.

The Task 46 under IEA Wind TCP is designed to improve understanding of the drivers of LEE, the geospatial and temporal variability in erosive events; the impact of LEE on the performance of wind plants and the cost/benefit of proposed mitigation strategies. Furthermore Task 46 seeks to increase the knowledge about erosion mechanics and the material properties at different scales, which drive the observable erosion resistance. Finally, the Task aims to identify the laboratory test setups which reproduce faithfully the failure modes observed in the field in the different protective solutions.

This report is a product of Work Package 4 **Laboratory testing of erosion.**

The objectives of the work summarized in this report are to:

- Provide a general introduction and explanation of the underlying functions and assumptions used in the lifetime tool published as part of D4.3, which can be found at https://gitlab.windenergy.dtu.dk/jaensi1/leading-edge-erosion-lifetime-calculations .
- Offer a high-level summary of the functionality and methodology behind converting rain erosion test results into turbine lifetime predictions.
- Explain how the assumptions made in laboratory testing are applied to predict erosion performance and lifetime of wind turbine blades in real-world conditions.

Table 1: IEA Wind Task 46 Participants.

Country	Contracting Party	Active Organizations
Belgium	The Federal Public Service of Economy, SMEs, Self-Employed and Energy	Engie
Canada	Natural Resources Canada	WEICan
Denmark	Danish Energy Agency	DTU (OA), Hempel, Ørsted A/S, PowerCurve, Siemens Gamesa Renewable Energy
Finland	Business Finland	VTT
Germany	Federal Ministry for Economic Affairs and Energy	Fraunhofer IWES, Covestro, Emil Frei (Freilacke), Nordex Energy SE, RWE, DNV, Mankiewicz, Henkel
Ireland	Sustainable Energy Authority of Ireland	South East Technology University, University of Galway, University of Limerick
Japan	New Energy and Industrial Technology Development Organization	AIST, Asahi Rubber Inc., Osaka University, Tokyo Gas Co.
Netherlands	Netherlands Enterprise Agency	TU Delft, TNO
Norway	Norwegian Water Resources and Energy Directorate	Equinor, University of Bergen, Statkraft
Spain	CIEMAT	CENER, Aerox, CEU Cardenal Herrera University, Nordex Energy Spain
United Kingdom	Offshore Renewable Energy Catapult	ORE Catapult, University of Bristol, Lancaster University, Imperial College London, Ilosta, Vestas
United States	U. S. Department of Energy	Cornell University, Sandia National Laboratories, 3M

Contents

List of Figures

List of Tables

Executive Summary

This report, a product of Work Package 4 (WP4) under IEA Wind Task 46, focuses on converting Rain Erosion Test (RET) data into actionable predictions for wind turbine blade lifetimes using the developed lifetime tool.

Key objectives include:

Tool overview: The report explains the functionality of the lifetime tool. The tool is accessible at https://gitlab.windenergy.dtu.dk/jaensi1/leading-edge-erosion-lifetime-calculations

The tool converts RET results into turbine lifetime predictions by integrating laboratory data with field conditions.

Methodology: The report provides details on the approach for deriving VN curves (velocity-to-number-of-impacts) from RET data and applying rationalized metrics to ensure consistency across tests.

Application: The report demonstrates how the tool incorporates damage accumulation models, with options for constant, probabilistic, or time-series-based scenarios, to predict blade lifetimes under varying rain and wind conditions.

The lifetime tool offers a systematic method to bridge laboratory testing and real-world performance, improving the accuracy of turbine lifespan predictions and informing effective erosion mitigation strategies.

1 Introduction

Erosion of wind turbine blades is generally simulated on a laboratory scale using a pressurized single-impact water gun or a three-specimen whirling arm apparatus subjugated to a distributed rain field. The whirling arm apparatus will be the subject of investigation. The whirling arm apparatus Rain Erosion Tester (RET) is "basically" a horizontal rotor with three arms, including a shower head with numerous needle-shaped nozzles, as exhibited in Figure 1.

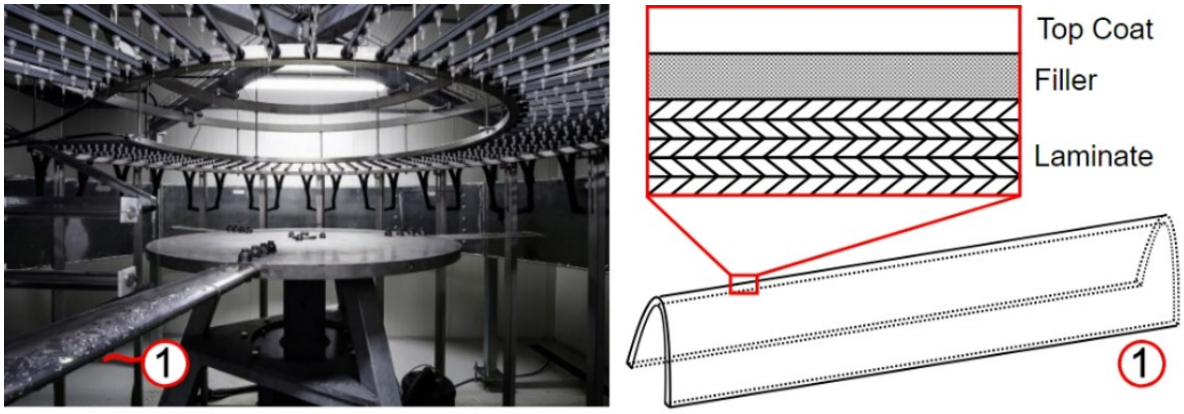

Figure 3: Illustration of a whirling arm rain erosion tester, with a coupon sized specimen indicated with (1) (left). Classical RET specimen and closeup depicting laminate, filler, and coating (right).

Before testing, the operator typically chooses an interval (every n-amount of minutes) at which point rain field is turned off and the rotor decelerates. Upon deceleration, a camera mounted inside the test chamber captures an image of the sample's surface. These images are then used to determine whether any material has been removed due to liquid droplet impact, by accessing the type of damage as classified in [20] and the radial location of the damages.

For the following rain field calculations the relevant measurement positions along with the values representative of typical for an operational R&D A/S RET is shown in Figure 2. The RET operator will have to know the parameters listed in Table 2.

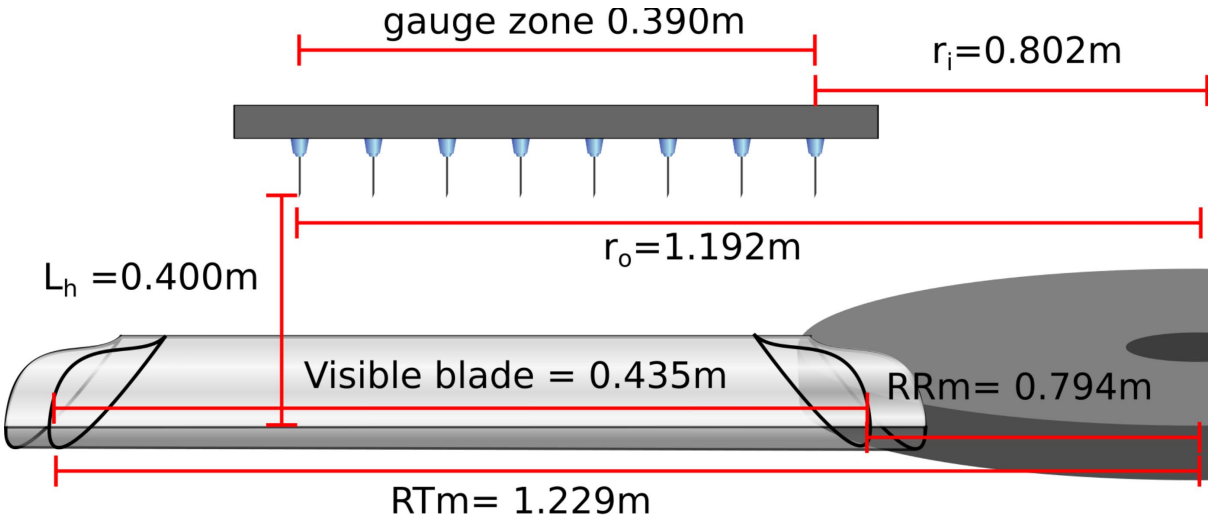

Figure 4: The illustration shows the relevant measurement positions with values representative of what is typically found in a operational R&D A/S RET. This illustration is adapted from [15].

Table 2: Required parameters to determine the impact velocity, accumulated flow, impingement and number of specific impacts pr. area.

Droplet size [m]	Droplet falling height [m]	Outer needle radius [m]	Inner needle radius [m]
d	L_h	r_o	r_i
ROI tip [m]	ROI root [m]	ROI tip [pixels]	ROI root [pixels]
RT_m	RR_m	RT_p	RR_p
RPM	Image slicing time [s]	Flow rate [L/h]	
Ω	t	F	

1.1 Rationalizing the impinged rain

When discussing the rationalization of impinged rain, the goal is to develop metrics that allow us to transfer and compare results not only between individual test runs but also between different machines. Ultimately, the aim is to apply the results from the lab to real-world conditions and use them to predict the lifetime of the leading-edge protection system.

Therefore, the objective is to convert test time by using machine parameters, as listed in Table 3, to obtain a robust rationalization of the impinged rain load. The following is not intended to be an exhaustive walkthrough of each rationalization; for more details, please refer to [1,2,4,15,17,18,19].

Table 3. Rain erosion test parameters.

Non-dimensional impacts	Impacts pr unit area	Impingement
Y_{N^*}	Y_N	Y_H

Using the methodology from ASTM G73-10 the first step is to calculate the volume concentration ψ:

$$\psi = \frac{U_r}{v_d}$$

where U_r is the rain rate and v_d is the velocity of the water normal to the blade. We see that this is a non-dimensional fraction representing the amount of any given volume of water. An example a rain shower with U_i of 10 mm/h and a fall velocity of 10 m/s

$$\psi = \frac{10[mm/h]}{10[m/s]} = \frac{2.78 * 10^{-6}[m/s]}{10[m/s]} = 2.78 * 10^{-5}\%$$

We see that for even a relative intense rain event only $2.78 * 10^{-5}\%$ of any given volume of air is water. To calculate the amount that hits a surface traveling normal to the falling droplet we calculate the total impingement H:

$$H = \psi * v_{blade} * t[m]$$

H represents the height in meters of the water column that has impacted the blade at the given velocity. Without going into further detail, the impingement in an R&D A/S RET, can be calculated with the following equation:

$$Y_H = \frac{F\omega t}{2\pi(r_0^2 - r_i^2) \cdot v_d}$$

It is important to note that all units should be in base SI, $\omega[rad/s]$ is the angular velocity is calculated from RPM. By the design of the RET, the impingement remains constant along the length of the test specimen.

The second rationalization is based on the Springer model's constant exponent of -5.7, as seen in Springer's 1976 book [19], page 45, figures 2-5. Here, it is assumed that droplets can be summed to affect their projected area and that these non-dimensional impacts fall on a single slope with a single exponent. In simpler terms, for a homogeneous material, there is no observed effect of droplet size.

$$Y_{N^*} = \frac{F \cdot \omega \cdot t}{\pi \cdot (r_0^2 - r_i^2) \cdot v_d} \cdot \frac{3}{2d}$$

The final rationalization to consider is impacts per unit area Y_N. This rationalization is only of use when input of results from RET testing into the Springer's semi-analytical model:

$$Y_N = \frac{F\omega t}{2\pi(r_0^2 - r_i^2) \cdot v_d} \cdot \frac{4}{3} \cdot \pi \cdot r^3$$

This can be used for example Springer's model for homogenous materials:

$$Y_N = 7 \times 10^{-6} \left(\frac{S}{P}\right)^{5.7} \cdot \frac{4}{\pi d^2}$$

where we know:

$$A_p = \frac{4}{\pi d^2}$$

The projected area A_p of a droplet of diameter d.

As such Y_n impacts per unit area **should not be used** on their own to compare coating performance, due to the sensitivity to any deviation in the assumed droplet diameter, which affects the final number of impacts. Instead, they should only be used as input for other models of impingement, like Springer or derivatives [1,2].

2 RET annotation

Annotation of damage points on rain erosion test samples depends on the metric used. It can be split into two distinct phases, denoted as incubation and breakthrough, see Figure 3.

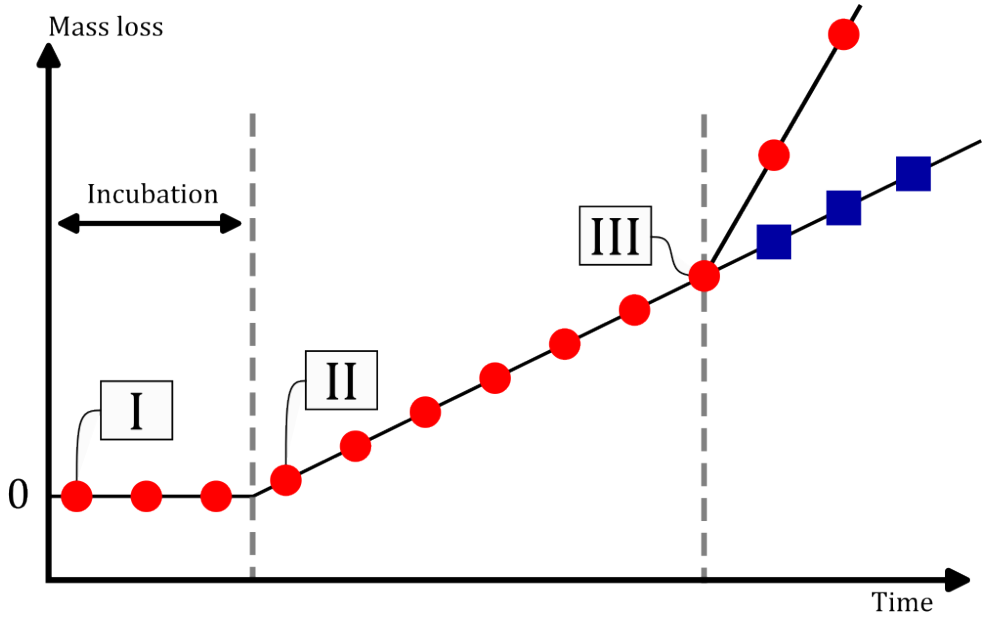

Figure 3: Evolution of a single damage point. (I) First sign of visible damage. (II) End of incubation. (III) Breakthrough to the substrate layer. The blue squares represent cases where no breakthrough occur.

Due to the subjective nature of the annotation process, identifying and noting consistent damage points requires significant expertise and systematic effort. The system's lifetime will vary depending on the metric used (incubation or breakthrough) (Johansen 2023 ref). It is essential to state what is meant by incubation or breakthrough. Henceforth, *incubation* is employed to specify the first sign of observable damage in the specimens. Data points obtained through continuous annotation of a set of samples subjected to different RPMs can then be plotted on a single graph, as depicted in Figure 4. The purpose is to generate a velocity to number of impact curve, analogous to SN curves in classical fatigue analysis.

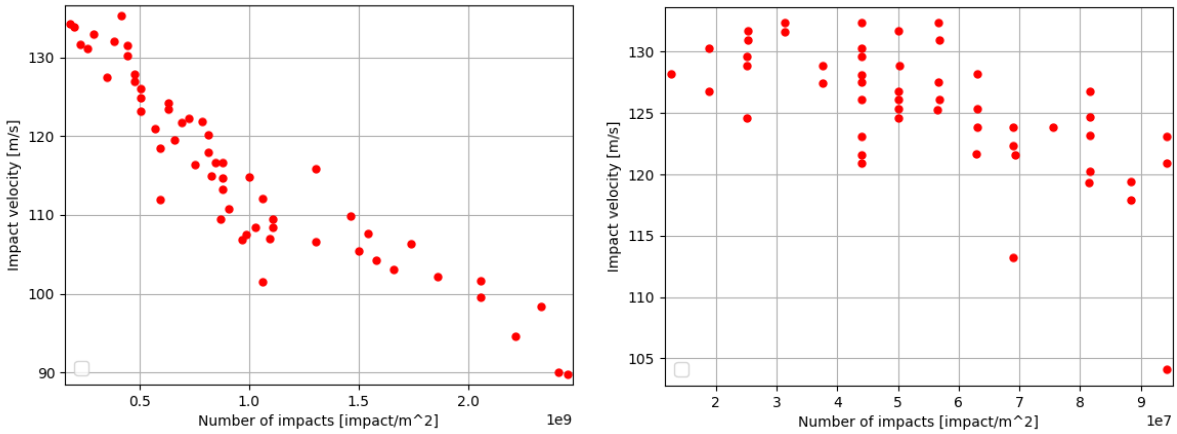

Figure 4: Data points for end of incubation visualized for two different coating systems.

Each of the curves in Figure 4 are shown with number of impacts. Alternatively, the x-axis values could have been expressed in terms of accumulated flow or impingement.

Evaluation of mass loss to determine the end of incubation requires specimen detachment and weighing. The localized erosion points can occur at multiple locations simultaneously; therefore, as noted by [1,2], it is not possible to determine the damage point associated with mass loss.

The probability of capturing an image upon the first sign of visible damage, incubation, or breakthrough is highly unlikely, as upon de-acceleration of the rotor, the water flow is turned off, indicating that damage occurs between two consequent images.

3 Regression approach and tolerance bands

3.1 Dependency

The data retrieved from the RET are assumed to follow a power law [1,2], expressed as Y- or X-dependent. Y- is referring to the second axis and X- is referring to the first axes on a fatigue curve. The recommended practice [1] for the choice of dependent parameters is the N-depend fit. However, as will be shown this can have a negative influence on regression results.

$$Y = C_1 X^{m_1} \rightarrow X = \left(\frac{Y}{C_1}\right)^{\frac{1}{m_1}}$$ *Y-dependent or V-dependent*

$$X = C_2 Y^{m_2} \rightarrow Y = \left(\frac{X}{C_2}\right)^{\frac{1}{m_2}}$$ *X-dependent or N-dependent*

where m and C are the power slope coefficient and adjustment coefficient, respectively.

3.2 Fitting procedure

Using the power-law as a prediction function, the model can be fitted in log10-space as follows:

$$X_{\log} = \log10(X),\ \ Y_{\log} = \log10(Y)$$

The power exponent or slope can be according [3] described as

$$m_1 = \frac{\sum_{i=0}^{n}\left(X_{\log,i} - X_{\log,mean}\right)\left(Y_{\log,i} - Y_{\log,mean}\right)}{\sum_{i=0}^{n}\left(X_{\log,i} - X_{\log,mean}\right)^2}$$

$$m_2 = \frac{\sum_{i=0}^{n}\left(Y_{\log,i} - Y_{\log,mean}\right)\left(X_{\log,i} - X_{\log,mean}\right)}{\sum_{i=0}^{n}\left(Y_{\log,i} - Y_{\log,mean}\right)^2}$$

and the adjustment coefficients are

$$C_1 = 10^{\left(Y_{\log,mean} - m_1 \cdot X_{\log,mean}\right)}$$
$$C_2 = 10^{\left(X_{\log,mean} - m_2 \cdot Y_{\log,mean}\right)}$$

The fitting procedure, choosing either of the dependencies are depicted in Figure 5.

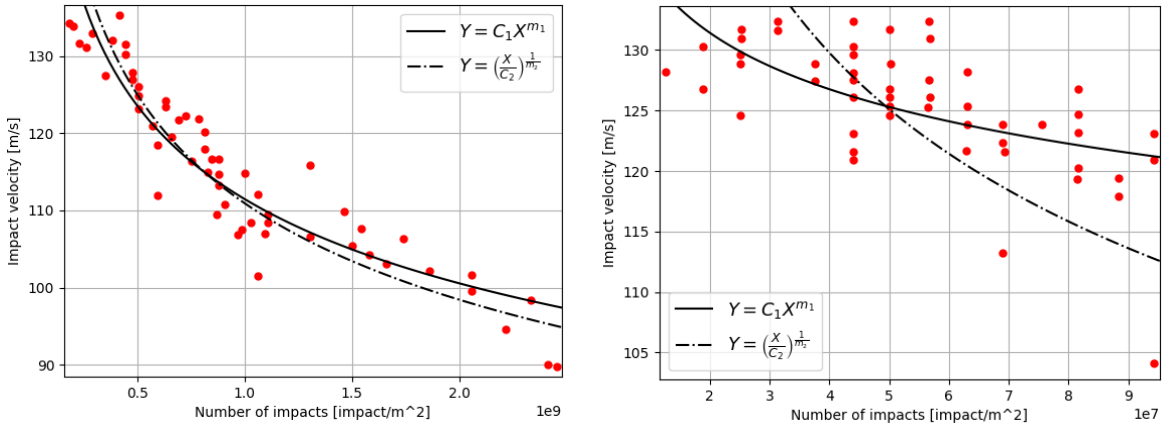

Figure 5: Illustrating the X- and Y-dependent fits on whirling arm rain erosion test data. The notation X- in this scenario is a reference to the number of impacts on the X–axis. The notation Y in this scenario is a reference to the impact velocity on the Y–axis.

For convenience we might at times choose to rearrange the V-dependent fit as if it's the N-depend fit, especially we comparing m exponents like Springer's m=-5,7.

$$Y = C_1 * X^{m_1} \rightarrow X = \left(\frac{1}{C_1}\right)^{\frac{1}{m_1}} * Y^{\frac{1}{m_1}}$$

When fitting V-dependent the equivalent C_e and m_e coefficients to compare directly to the standard N-dependent fit are:

$$C_e = \left(\frac{1}{C_1}\right)^{\frac{1}{m1}} \qquad m_e = \frac{1}{m1}$$

3.3 Tolerance bands

A tolerance band states that a certain percentage of the data lies within or above the prediction statement. It is typically interesting to identify the lower limits in which 75- and 95 % of the data are above the prediction statement to estimate a conservative measure of the blade lifetime. Several methods exist to identify these limits, such as assuming the data follows a normal- or Weibull distribution as described in [16].

The distribution-based methods tend to yield confidence that are not representative of the recoded data points, especially for high number of data points often result in very narrow confidence bands. The choice was therefore made to calculate the distribution's upper- and lower quantiles so that it remains true to the data points, e.g. if there is 100 data-points, 95 data-points are above the 95% line and so forth. Figure 6 depicts the tolerance bands for the two different coating systems.

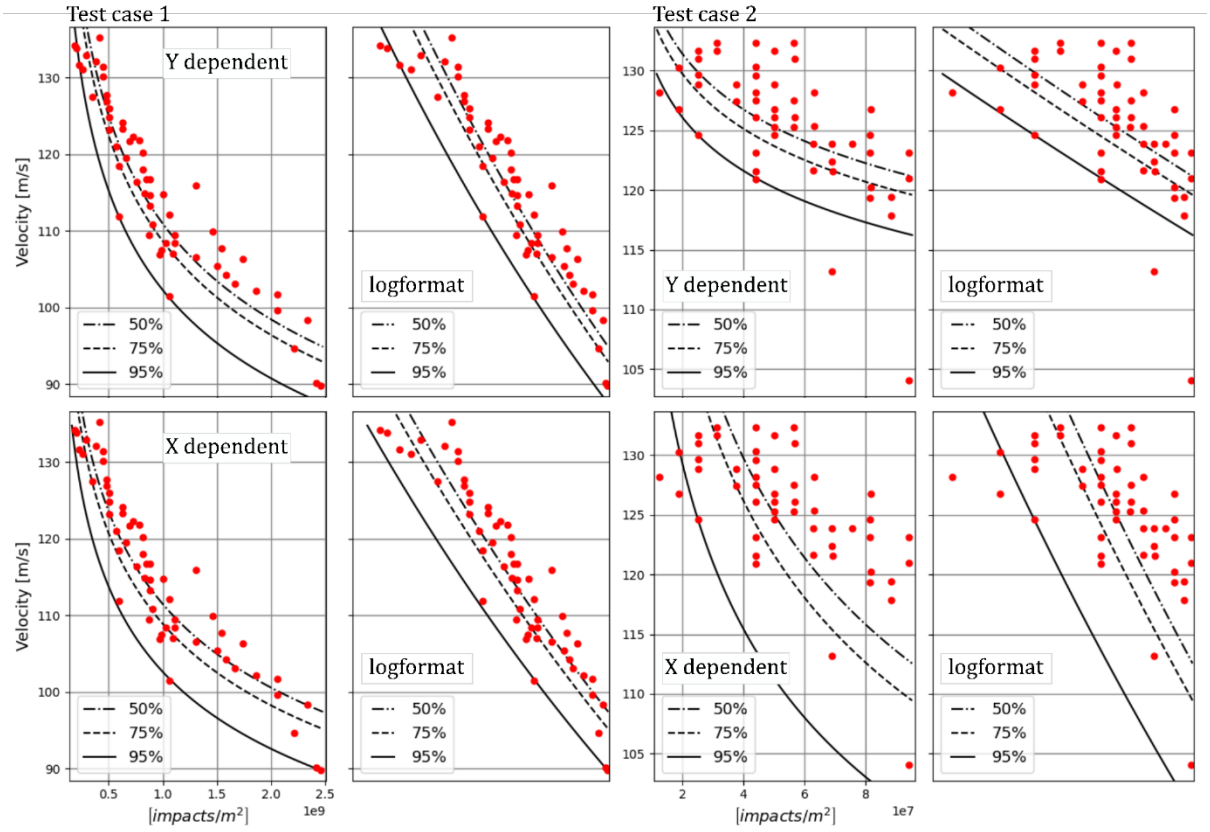

Figure 6: Illustration of the 50, 75 and 95 % tolerance limits using the normal and logscale for two different test case coatings using (upper panels) Y-dependent method, and (lower panels) X-dependent method.

The output from the algorithm is two new adjustment coefficients that account for the tolerance limits, mathematically stated as

$$Y_{75} = C_{1,75}X^{m_1}, \;\; Y_{75} = \left(\frac{X}{C_{2,75}}\right)^{\frac{1}{m_2}}$$

$$Y_{95} = C_{1,95}X^{m_1}, \;\; Y_{95} = \left(\frac{X}{C_{2,95}}\right)^{\frac{1}{m_2}}$$

The fitting procedure, choosing either of the dependencies, yields two different results, as depicted in Figure 4. In summary we note:

- The V-dependent fit is closer to data points at low velocities
- The N-dependent fit is closer to data points at higher velocities
- The discrepancy between the two fits is due to the sum of squared differences relative to the mean computed in the denominator of the slope coefficient.
- Scatter can be observed in Figure 4 on both velocity and number of impact curves.

4 Damage accumulation.

To relate rain erosion testing to field conditions, it is necessary to know the wind speed and precipitation conditions at the site of interest. Rain impingement relates to liquid (rain) precipitation. The rainfall rate is typically measured in millimetres per second, minute, hour, day, or year.

The rainfall should always be converted to the units' equivalent of those describing the RET fatigue curve, defined in Section 1. In computing the damage, we use the power law describing the velocity to number of impacts curve as our reference value. We, therefore, state that for either of the dependencies

$$X_i = \left(\frac{Y}{C_1}\right)^{\frac{1}{m_1}} \;\; or \;\; X_i = C_2 Y^{m_2}$$

The above adjustment coefficient can easily be interchangeable with the 75 and 95 % tolerance limits.

Below we give three examples on how to calculate the number of years to end of incubation using the same meteorological wind speed and rainfall input for all three examples. In the first, we assume the average wind speed and average rainfall is all that is known. In the second, we assume the distribution of wind speed and the distribution of rainfall exist are known and probabilistic approach is applied. In the third, we assume the wind speed and rainfall are dependent using a time-series approach. The results in the scenarios demonstrate how the tool incorporates

damage accumulation models, with options for constant, probabilistic, or time-series-based scenarios, to predict blade lifetimes under varying rain and wind conditions.

4.1 Scenario 1: Constant wind speed and rain intensity

The simplest damage accumulation method assumes the yearly amount of rain is constant and the turbine is rotating with a constant RPM all year. The impact rate the blade experiences in the field can be expressed as a single value:

$$X_j \ [impacts/m^2/s]$$

In using the Palmgren-Miner's damage accumulation rule it can be stated that fatigue failure occurs when damage *D* exceeds one:

$$D = \frac{X_j}{X_i} \ [1/s \ ]$$

To equate the number of years we invert the damage parameter as such

$$\Gamma = \frac{1}{D}(365 \cdot 24 \cdot 60 \cdot 60)$$

4.2 Scenario 2: Probabilistic wind speed and rain intensity

The second option is to correlate the turbine speed to the rainfall rate as depicted in figure 6. This is a probabilistic approach for the damage modelling.

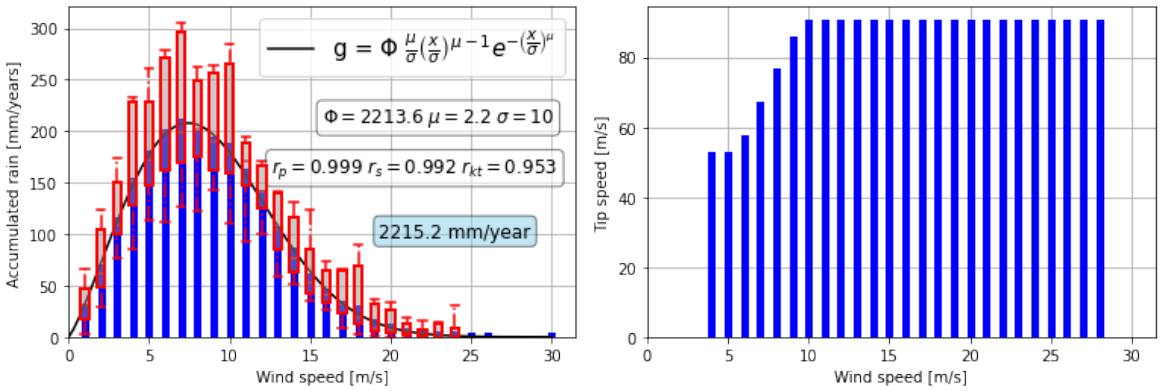

Figure 7: The area under the left curve is the total amount of rain the specific turbine will experience in one year. The red box and upper bounds are the min, max, median, and upper and lower quantiles. The left and right curves can be correlated through the wind speed bins.

In this scenario, the damage varies relative to the blade tip speed and rain conditions. Employing Palmgren-Miner's damage accumulation rule, it can be stated that

$$D = \sum_{i,j=0}^{n} \frac{X_j}{X_i} = \frac{X_{j=1}}{X_{i=1}} + \frac{X_{j=2}}{X_{i=2}} + \cdots + \frac{X_{j=n}}{X_{i=n}}, \quad X_j \neq X_i \quad \text{for } i = j$$

Where *n* is the number of windspeed bins seen in Figure 7. To equate the number of years, we invert the damage parameter as such

$$\Gamma = \frac{1}{D}(365 \cdot 24 \cdot 60 \cdot 60)$$

4.3 Scenario 3: Time-series wind speed and rain intensity

The third option is to use a time-series based approach, where each increment in rainfall from the time-series is contributing to the total damage sum for the specific wind speed, see Figure 8.

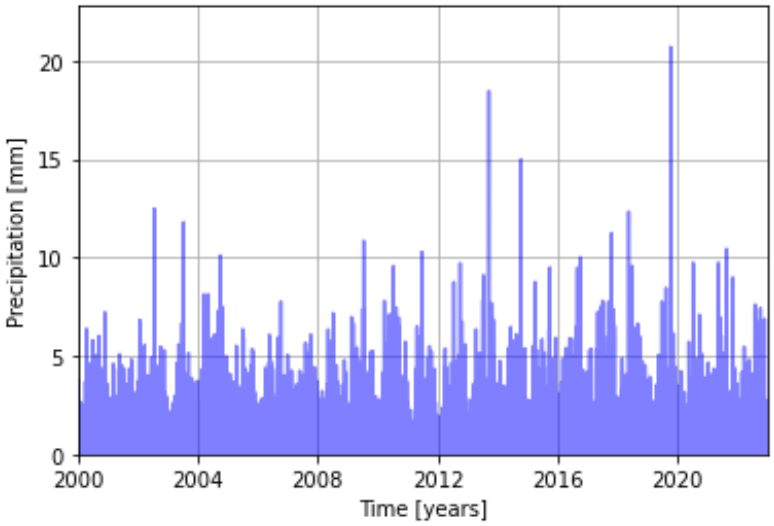

Figure 8: An example of precipitation time series, with a temporal resolution of 1 hour and recorded over 22 years.

In using Palmgren-Miner's damage accumulation rule it can be stated that

$$D = \sum_{i,j=0}^{m} \frac{X_j}{X_i} = \frac{X_{j=1}}{X_{i=1}} + \frac{X_{j=2}}{X_{i=2}} + \cdots + \frac{X_{j=n}}{X_{i=n}}, \quad X_j \neq X_i \quad \text{for } i = j$$

where *m* is the number of increments in the time series. To equate the number of years we invert the damage parameter as such

$$\Gamma = \frac{1}{D} N_{\text{years}}$$

Where N_{years} is the number of years in the time-series.

Scenario 1 does not account for situations where rain impacts at or below rated speed, thus reducing the damage increment. Only average wind speed and average rainfall is needed for the calculation.

Scenario 2 may be applied in case long-time series rain intensity and wind speed data are not available.

Scenario 3 is the most comprehensive of the three methods and it requires long-term time series of rain intensity and wind speed.

The Palmgren-Miner damage accumulation rule assumes that the loading history is periodic with a constant amplitude. It is argued that the droplets are evenly dispersed along the gauge length, hitting the specimen simultaneously without the influence of turbulence or clotted needles.

Each of the three described scenarios can employ several additional assumptions, such as the inclusion of a material model, variable droplet sizes, and velocity profiles – as done in [4,5,6,7,8].

5 Key conclusions and recommendations

The influence of an annotator's subjectivity on damage evaluation of eroded coating samples can be decreased by introducing changes to the workflow described by DNV-GL, as suggested in [9]. It was found that using advanced image analysis techniques to track a single erosion point from the first sign of visible damage to breakthrough will leverage the full evolutionary damage process to establish a mathematical/model expression, allowing the determination of an exact end of incubation and breakthrough value.

When using the VN curve obtained from whirling arm rain erosion testing, assuming a constant rate of flow, droplet size, and velocity as a comparable reference can lead to errors. Realistic field conditions are highly variable, and this discrepancy highlights the limitations of our current testing standards.

Polymers are per nature temperature- and rate-dependent, meaning that different operative conditions can influence end failure. From a VN-regression-based viewpoint, you may see one failure mode in the high-velocity regime (relative based on the testing region) compared to the low-velocity regime. One could, therefore, imagine that two or more slopes would be present in the failure data obtained from testing instead of one, as currently described by the recommended practice [1,2,3].

The current standard [3] only accounts for a single dependency, which leads to a discrepancy in the data of the desired direction. It is common practice to conduct accelerated testing and extrapolate to the desired application range, but this potentially results in a significant difference between the X- and Y-dependent methodologies. To address the problem, it is crucial to utilize a more comprehensive regression standard to incorporate the error in both directions, such as orthogonal regression or deming regression [10,11] or a multiple slope approach that adjusts the prediction statement based on a set of N-number local errors [12,13,14].

Unfortunately, the scatter in the RET data is a reoccurring problem caused by manufacturing-induced defects and material heterogeneities. Manufacturing will always be prone to error, especially when viewed from the perspective of offshore turbines with a rotor span of 220 meters. It is therefore recommended to test LEPs with pre-induces defects, at realistic tip speeds to investigate the critical length scale for damage initiation.

6 References

[1] DNVGL: RP-0171. *Testing of Rotor Blade Erosion Protection Systems: Recommended Practice*; DNV GL: Oslo, Norway, 2018
http://www.dnvgl.com

[2] DNV-RP-0573, Evaluation of erosion and delamination for leading edge protection systems of rotor blades
https://standards.dnv.com/explorer/document/

[3] Standard Practice for Statistical Analysis of Linear or Linearized Stress-Life (S-N) and Strain-Life (ε-N) Fatigue Data - ASTM E739-10 2015.

https://www.astm.org/e0739-10r15.html

[4] Experimental study on the effect of drop size in rain erosion test and on lifetime prediction of wind turbine blades – Bech et al 2022.
https://www.sciencedirect.com/science/article/pii/S0960148122009673.

[5] Evaluation of wind turbine blades' rain-induced leading edge erosion using rainfall measurements at offshore, coastal and onshore locations in the Netherlands - Caboni et al. 2024
https://iopscience.iop.org/article/10.1088/1742-6596/2767/6/062003

[6] A probabilistic long-term framework for site-specific erosion analysis of wind turbine blades: A case study of 31 Dutch sites – Verma et al 2021.
https://onlinelibrary.wiley.com/doi/10.1002/we.2634

[7] Impact of meteorological data factors and material characterization method on the predictions of leading edge erosion of wind turbine blades – Caboni et al. 2024
https://doi.org/10.1016/j.renene.2024.120549

[8] The size distribution of raindrops – Best.
http://dx.doi.org/10.1002/qj.49707632704

[9] Improved detection for leading edge damage informed by rain erosion facility experiments – Jastrzebski 2024.
https://findit.dtu.dk/en/catalog/66b40cd0a645ebe8f3b850d1

[10] Deming regression, MethComp package – Jensen 2007.
online_pdf

[11] Julius Weisbach's pioneering contribution to orthogonal linear regression – Dietrich et al. 2018
https://doi.org/10.1016/j.hm.2017.12.002

[12] An improved model for predicting the scattered S-N curves. Klemenc et al. 2015
https://www.svjme.eu/search/?search=An+improved+model+for+predicting+the+scattered+S-N+curves

[13] Joint estimation of E–N curves and their scatter using evolutionary algorithms Klemenc et al. 2013.
https://doi.org/10.1016/j.ijfatigue.2013.08.005

[14] Essential structure of S-N curve: Prediction of fatigue life and fatigue limit of defective materials and nature of scatter. Murakami et al. 2021.
https://doi.org/10.1016/j.ijfatigue.2020.106138

[15] Fæster, S., Johansen, N. F. J., Mishnaevsky, L., Kusano, Y., Bech, J. I., & Madsen, M. B. (2021). Rain erosion of wind turbine blades and the effect of air bubbles in the coatings. Wind Energy. https://doi.org/10.1002/we.2617

https://doi.org/10.1002/we.2617

[16] ASTM E739 − 10. (2012). Standard Practice for Statistical Analysis of Linear or Linearized Stress-Life (S-N). Annual Book of ASTM Standards, i(Reapproved), 1–7. https://doi.org/10.1520/E0739-10.2

[17] ASTM. (2017). ASTM G73 - 10 (Reapproved 2017) Standard Test Method for Liquid Impingement Erosion Using Rotating Apparatus1. https://doi.org/10.1520/G0073-10R17

[18] Leading, B., Protection, E., & Johansen, N. F. (n.d.). Test Methods for Evaluating Rain Ero- sion Performance of Wind Turbine Blade Leading Edge Protection Systems Nicolai Frost-Jensen Johansen PhD Thesis Test Methods for Evaluating Rain. https://orbit.dtu.dk/files/236330239/PHD_thesis_Nicolai_Frost_Jensen_Johansen.pdf

[19] Springer, G. S. (1976). Erosion by Liquid Impact. In Scripta Publishing Co. a division of Scripta Technica, Inc. Scripta Publishing Co. a division of Scripta Technica, Inc.

[20] Johansen, N. F.-J., 2023 Erosion failure modes in leading-edge systems. IEA Task 46 deliverable. https://iea-wind.org/wp-content/uploads/2023/06/IEA-WT46-WP4.2-Erosion-failure-modes-in-leading-edge-systems.pdf